Article

Journal of the Brazilian Chemical Society

https://dx.doi.org/10.21577/0103-5053.20240139

J. Braz. Chem. Soc. **2024**, *35*, 12, e-20240139, 1-9

Adsorption Kinetics of Tartrazine Dye on Activated Carbon Derived from Guava (*Psidium guajava*) Seeds

Elinei N. C. de Almeida,[a] Erlan A. Pacheco,[a] Koji J. Nagahama,[b] Tereza Simonne M. Santos[b] and Alexilda O. de Souza *,[a]

[a]*Programa de Pós-Graduação em Química, Laboratório de Catálise e Química dos Materiais, Universidade Estadual do Sudoeste da Bahia, 45700-000 Itapetinga-BA, Brazil*

[b]*Programa de Pós-Graduação em Engenharia Civil e Ambiental, Universidade Estadual de Feira de Santana, Av. Transnordestina, s/n, Novo Horizonte, 44036-900 Feira de Santana-BA, Brazil*

Azo dyes are widely used in various industries. However, many of these dyes are carcinogenic and reduce light penetration into aqueous systems, posing a threat to human health and hampering photosynthesis in aquatic environments. In this study, guava seeds were used to produce activated carbon by chemical activation with $ZnCl_2$. The carbon was characterized and used as an adsorbent to remove tartrazine dye in aqueous medium. X-ray diffraction showed the formation of a material with disordered graphitic planes, typical of activated carbons. The equilibrium time for the dye-activated carbon system was found to be 80 min by the Southwell plot method. The adsorbent removed 97.6% of the dye, representing an adsorbed concentration of 1.62 mg g^{-1} for an adsorbent dosage of 12 g L^{-1}. The pseudo-second-order and Elovich kinetic models provided the best fit to experimental data, suggesting that chemisorption is the predominant mechanism, combined with the effect of surface heterogeneity. From an environmental point of view, the results suggest that the activated carbon produced is an efficient material for the treatment of industrial wastewater containing azo dyes.

Keywords: azo dye removal, kinetic studies, southwell plot method, biomass, activated carbon

Introduction

Environmental pollution has worsened in recent decades as a result of the increased disposal of contaminants into the environment, driven by population growth and the intensification of industrial activities. Despite the existence of laws mandating waste and wastewater treatment, many industries fail to comply with such requirements. Thus, inadequate discharge of organic compounds such as pesticides, drugs, and dyes by different industrial sectors is currently one of the main causes of pollution of water resources.[1-4]

Given their complex structure, high chemical stability, and low biodegradability, dyes have a high potential to contaminate water resources.[1,5,6] Synthetic dyes, particularly those with an azo group linked to an aromatic ring, cannot be efficiently removed by conventional treatment methods. Conventional methods also have important drawbacks. For instance, coagulation and flocculation generate large quantities of sludge at the end of the process, whereas oxidation, ion-exchange, and membrane separation have high cost, high energy consumption, and the potential to form toxic by-products.[7-9] On the other hand, adsorption has been widely applied in dye removal. This technique stands out for its high efficiency and environmental friendliness, as it generates low amounts of waste and enables adsorbent reuse.[10-13]

Activated carbons are the most commonly used adsorbents for the removal of contaminants in aqueous media. The popularity of these materials stems from their high specific surface area, porous structure, thermal and chemical resistance, and presence of a broad variety of functional groups that can provide acidic, basic, or neutral characteristics.[6,8,11,14,15] However, commercially available activated carbons are expensive, which makes their large-scale application unfeasible. In light of this, many studies[16-22] investigated the production of low-cost and

*e-mail: alexilda@uesb.edu.br
Editor handled this article: Aldo José Gorgatti Zarbin (Guest)

efficient activated carbons as an alternative to commercial charcoals. The use of agroindustrial residues for the production of activated carbon has gained prominence, as these materials are generated in large quantities, have a high carbon content, and contain a low percentage of inorganic compounds.[16-22]

In view of the foregoing, this study aimed to prepare activated carbon from guava seeds and investigate its potential as an adsorbent of azo dyes in aqueous medium. Thus, in addition to producing a low-cost adsorbent and adding value to the waste material, this study contributes to reducing the environmental impacts caused by inadequate disposal of organic waste into the environment.

Experimental

Preparation of activated carbon

Guava processing waste was kindly provided by a fruit pulp agroindustry in Bahia State, Brazil. The material was washed under water to remove impurities, dried in the sun for 48 h, and dried in an air-circulation oven at 60 °C for 24 h. After drying, the seeds were sieved to ensure the complete removal of pulp residues, ground in a knife mill equipped with a 2 mm screen, and manually mixed with $ZnCl_2$ (ACS, São Paulo, Brazil) solution at a 2:1 (residue/activator) ratio. The mixture was homogenized and distilled water was added to form a paste, which was oven-dried at 100 °C for 48 h. Subsequently, the material was calcined for 2 h in a muffle furnace (EDG, São Paulo, Brazil) at 600 °C with a heating ramp of 10 °C min^{-1} under inert atmosphere (N_2, 100 mL min^{-1}). The resulting activated carbon was washed with distilled water at 40 °C until the chloride test was negative and then oven-dried at 100 °C to obtain activated guava seed carbon (GSC).

GSC characterization

GSC was characterized by several techniques. Elemental analysis (CHNS) was performed using a EA3000-CHNS analyzer (Euro Vector, Pavia, Italy) with a TDC detector, and sulfanilamide as a reference standard. X-ray diffraction (XRD) pattern was recorded using a XRD D2 Phaser diffractometer (Bruker, Billerica, Massachusetts, USA) using Cu Kα radiation source (λ = 0.15418 nm), nickel filter, tube voltage of 30 kV, tube current of 10 mA, 2θ scan from 10 to 90° and scan speed of 2 degree min^{-1}. The Fourier transform infrared (FTIR) spectra was achieved using a Prestige-21 spectrometer (Shimadzu, Kyoto, Japan) in the range 4000-400 cm^{-1}, KBr pellets, and a resolution of 4 cm^{-1}. The scanning electron microscope (SEM) images were recorded to visualize the surface morphology of guava seed and activated carbon produced, using Phenom Pure equipment (Thermo Fisher Scientific, Waltham, Massachusetts, USA) with a backscattered electron detector, accelerating voltage of 5 kV, resolution < 15 nm, and magnification up to 175.000×.

Brunauer-Emmett-Teller (BET) specific surface area and pore properties were determined from N_2 adsorption data at 77 K using an ASAP 2020 system (Micromeritics, Norcross, Georgia, USA). Before adsorption measurements, the sample (0.3 g) was heated (10 °C min^{-1}) under nitrogen flow (60 mL min^{-1}) up to 160 °C (30 min). The specific surface area was calculated using the adsorption data in a range from 0.05 to 0.2 of relative pressure. The pore size distribution was determined through the Barret-Joyner-Halenda (BJH) mathematical model.

The point of zero charge (PZC) was measured using the methodology called "11 point experiment" by mixing 20 mg of activated carbon with 20 mL of 0.1 mol L^{-1} NaCl (Synth, São Paulo, Brazil) solutions in different flasks and adjusting the pH in the range from 2-12 with 0.1 mol L^{-1} HCl (Synth, São Paulo, Brazil) solution or 1 mol L^{-1} NaOH (Synth, São Paulo, Brazil) solution. The suspensions were maintained under stirring time of 24 h, filtered and the pH of the filtrate measured with the pH meter (HI9829-HANNA® instruments, São Paulo, Brazil). The PCZ was determined by plotting the graph of final pH *versus* initial pH and determining the range where the buffer effect was observed, that is, where the pH did not vary.[23,24]

Adsorption experiments

Adsorption capacity

For determination of adsorptive capacity, appropriate masses of GSC were directly weighed into 50 mL Erlenmeyer flasks on an analytical balance. Then, 25 mL of tartrazine solution at 20 mg L^{-1} were added and the pH was adjusted to the desired value (pH 6.10). All tubes were placed on an orbital shaker at room temperature. The entire procedure was carried out in triplicate. The quantification of tartrazine dye in the supernatant solution was performed by using a spectrophotometer (Shimadzu, UV-1280, Kyoto, Japan). An analytical curve (Figure S1, Supplementary Information (SI) section) of maximum absorbances at 430 nm was constructed and used to determine tartrazine concentrations and the final concentration of dye after adsorption. For this, tartrazine solutions were prepared at concentrations of 5.0, 10, 15, 20, 25, and 30 mg L^{-1}. A blank solution (without tartrazine) was also prepared.

Carbon adsorption capacity (q_e, mg dye g^{-1} adsorbent) was determined using equation 1:

$$q_e = \frac{(C_0 - C_e)}{m} \times V \quad (1)$$

where C_0 and C_e (mg L^{-1}) are the initial and final concentrations of the dye solution, respectively; m (g) is the mass of adsorbent, and V (L) is the volume of the dye solution. Removal capacity was also expressed as percentage, as shown in equation 2:

$$\text{Removal capacity}(\%) = \frac{(C_0 - C_e)}{C_0} \times 100 \quad (2)$$

Determination of experimental parameters

Adsorbent mass

The influence of adsorbent mass on dye adsorption was studied by adding different masses of activated carbon to the system. The following masses were investigated: 0.05, 0.10, 0.20, 0.30, 0.40, 0.50, 0.60, 0.70, 0.80, and 1.00 g. The adsorbent was weighed directly into Erlenmeyer flasks on an analytical balance, and 25 mL of dye solution at 20 mg L^{-1} were added. The entire procedure was performed in triplicate. Subsequently, the flasks were placed on an orbital shaker (16.0 rpm). The solutions were left in contact with the adsorbent for 3 h at room temperature (25 ± 1 °C). After this time, the solutions were filtered and immediately analyzed spectrophotometrically.

pH value

This step was performed to assess the influence of pH on tartrazine adsorption. Experiments were carried out using the adsorbent mass (0.3 g) that provided the best adsorption results in the previous step, following the same experimental procedures used to determine the adsorption capacity but with pH variation. The pH of 25 mL of tartrazine solution at 20 mg L^{-1} was adjusted by using 0.1 mol L^{-1} NaOH or HCl solution and a calibrated digital pH meter. The following pH values were investigated: 2.0, 3.0, 5.0, 7.0, 9.0, 10, and 11. The entire procedure was carried out in triplicate.

Adsorption kinetics

After optimization of the above-mentioned parameters, the time required for the adsorbent/adsorbate system to reach adsorption equilibrium was investigated. Batch adsorption experiments were carried out by varying the contact time between activated carbon and the tartrazine solution but maintaining the adsorbent mass and pH that resulted in the best adsorption results in the previous step.

Subsequently, 25 mL of the dye solution at 20 mg L^{-1} were added, and flasks were placed on an orbital shaker (16.0 rpm) at room temperature (25 ± 1 °C). While the solutions were kept under stirring, aliquots (3 mL) were taken from each flask at time intervals of 5, 10, 15, 20, 25, 40, 50, 60, 80, 100, 120, 140, 160, 180, 200, 220, and 240 min. The entire procedure was carried out in triplicate. After collection, the solutions were filtered and immediately quantified using a UV-Vis spectrophotometer.

The results of the kinetic study were treated by the Southwell plot method. Kinetic parameters were investigated by application of pseudo-first-order, pseudo-second-order, and Elovich kinetic models, according to the equations described in Table 1.

Results and Discussion

Characterization

The results of elemental analysis of guava seeds (GS) and GSC are presented in Table 2. There was an increase in carbon content, a decrease in hydrogen content, and complete elimination of sulfur, suggesting the occurrence of dehydration and decomposition reactions leading to the formation of a carbon-rich material. It was possible to note that the atomic H/C ratio of GSC is lower than that of the starting biomass (GS). This effect can be attributed to the loss of OH groups caused by dehydration and dehydrogenation, the breaking of weak hydrogen bonds within the coal structure, and the loss of volatile organic products. According to literature information,[18] this finding may also suggest aromatization of activated carbon.

Table 1. Some adsorption kinetic models

Name	Model	Linear form	Reference
Lagergren pseudo first-order model	$\frac{dQ}{dt} = K_1(Q_e - Q_t)$	$\log(Q_e - Q_t) = \log Q_e - \frac{k_1}{2.303} t$	25
Pseudo-second order model	$\frac{dQ_t}{dt} = K_2(Q_e - Q_t)^2$	$\frac{t}{Q_t} = \frac{1}{k_2 Q_e^2} + \frac{t}{Q_e}$	26
Elovich	$\frac{dQ_t}{dt} = \alpha \exp(-\beta q_t)$	$q_t = \beta \ln(\alpha\beta) + \beta \ln t$	27

Q_e and Q_t: adsorption capacities at equilibrium and at time *t*, respectively; K_1: pseudo-first-order adsorption rate constant; K_2: pseudo-second-order adsorption rate constant; α and β: Elovich parameters (α = initial sorption rate and β = desorption constant).

Table 2. Elemental analysis of guava seeds (GS) and activated guava seed carbon (GSC)

Sample	C / %	H / %	N / %	S / %	H/C
GS	41.9	4.6	0.6	0.5	1.3
GSC	60.0	2.4	1.8	–	0.5

C: carbon content; H: hydrogen content; N: nitrogen content; S: sulfur content; H/C: atomic hydrogen/carbon ratio.

XRD analysis showed a diffraction pattern characteristic of activated carbons and amorphous materials in general (Figure 1), with the absence of well-defined reflections and the presence of two amorphous halos, a more intense halo at 2θ ca. 24°, and a lower intensity halo at 2θ ca. 44°. These results suggest that the microcrystalline lignocellulosic constituents present in GS were transformed during pyrolysis into a disordered graphitic structure with a high carbon content (Table 2). The observed amorphous halos correspond to reflections of the (002) and (100) planes of microcrystalline graphite, respectively. The occurrence of these two broad reflections suggests an increase in the regularity of the crystalline structure, resulting in better alignment of graphitic planes.[28]

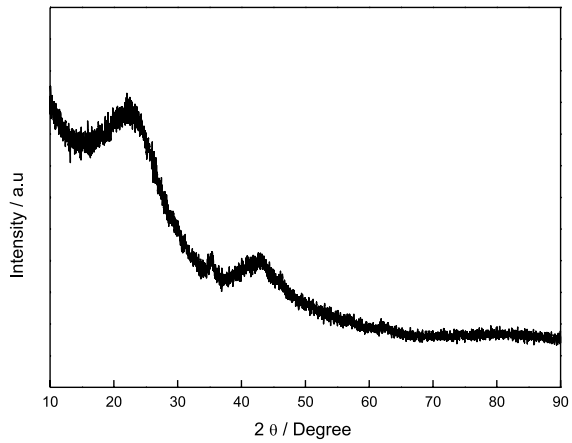

Figure 1. X-ray diffraction pattern of activated guava seed carbon produced (GSC).

It was also noted a low intensity reflection at 2θ value of 35° corresponding to the lattice plane (002) of the wurtzite hexagonal structure of ZnO (JCPDS file 36-1451), indicating that the activating agent was not completely removed during the washing step of GSC.

In the FTIR spectrum of activated carbon illustrated in Figure 2, the band at 3450 cm^{-1} is attributed to O–H stretching of alcohols and phenolic compounds. The band at 1635 cm^{-1} corresponds to C=C stretching of aromatic rings, which is typical of activated carbons. The vibrational mode observed at 1380 cm^{-1} may be attributed to C–O stretching of alcohols, phenols, and esters. Finally, the broad band at 800-400 cm^{-1} is characteristic of C–H deformation vibrations outside the plane of the aromatic structure.[5,28,29]

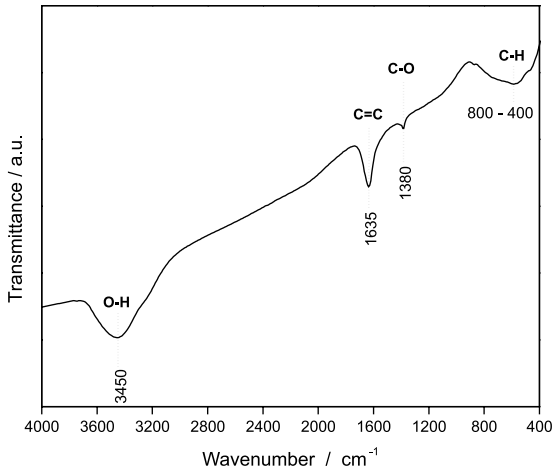

Figure 2. FTIR (KBr) spectra of the activated guava seed carbon produced (GSC).

Figure 3 shows the results of the experiment to determine the pH_{pzc}. pH_{pzc} is determined in the range where the buffering effect is observed, that is, where the pH does not vary. According to the results, the pH at which the activated carbon surface is neutrally charged (pH_{pzc}) is approximately 7.0.

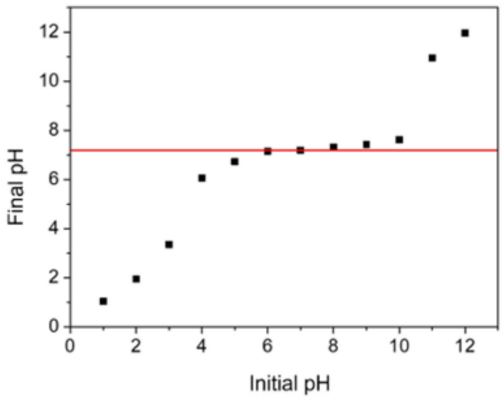

Figure 3. Determination of the pH of point zero charges on the surface of activated guava seed carbon produced (GSC).

When the solution is kept at a pH lower than the pH_{pzc} of activated carbon, certain functional groups are protonated, and the material behaves as a positively charged matrix, attracting the negatively charged ions present in the solution. On the other hand, when the solution pH increases, reaching values higher than the pH_{pzc}, the surface charge of activated carbon becomes negative and cation binding is favored, as active functional groups on the GSC surface are deprotonated.

The SEM images of guava seed and activated carbon are shown in Figure 4. It was possible to verify that the guava

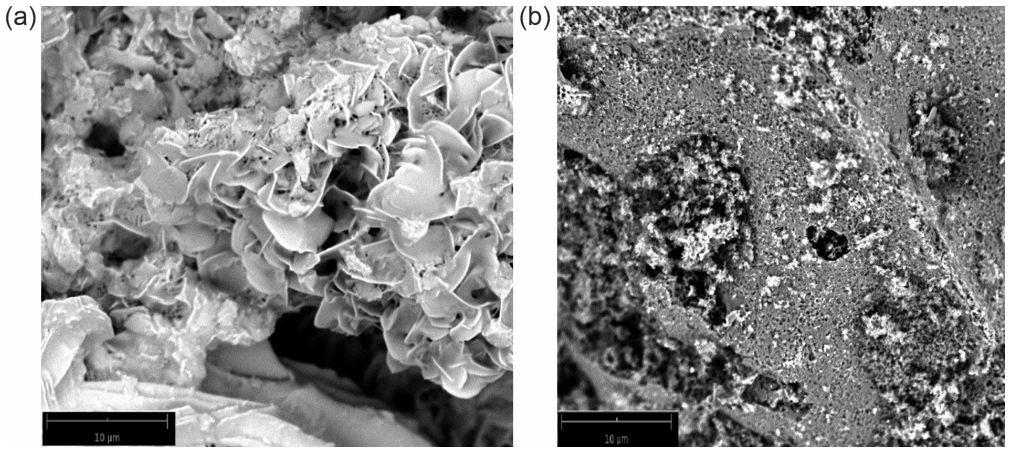

Figure 4. Surface morphology: (a) guava seed used as a precursor of activated carbon (GS) and (b) activated guava seed carbon produced (GSC).

seed (GS) presented a heterogeneous surface morphology, with porous aggregates, and some particles presented a smooth surface. The image of GSC showed a heterogeneous and porous surface that favors the adsorption process.

The results of textural properties shown by the GSC are described in Table S1 and Figure S2 (SI section). It was observed that the activated carbon exhibited a good value for a specific area (480 $m^2 g^{-1}$). The adsorption-desorption isotherm obtained (Figure S1) has a profile similar to type I of the International Union of Pure and Applied Chemistry (IUPAC) classification, characteristic of microporous materials.[30]

Adsorption studies

Adsorbent mass

The effect of adsorbent mass on dye removal is depicted in Figure 5. An adsorbent mass of 0.05 g led to a dye removal of 46.35%. When 0.1 g of adsorbent was used, removal increased by about 40%; when 0.2 g was used, a removal efficiency of 98.87% was achieved. From 0.3 to 1.1 g of adsorbent, there were no significant variations in adsorptive capacity, and the removal rate remained around 98%. Therefore, an adsorbent mass of 0.3 g was chosen for pH and kinetic studies.

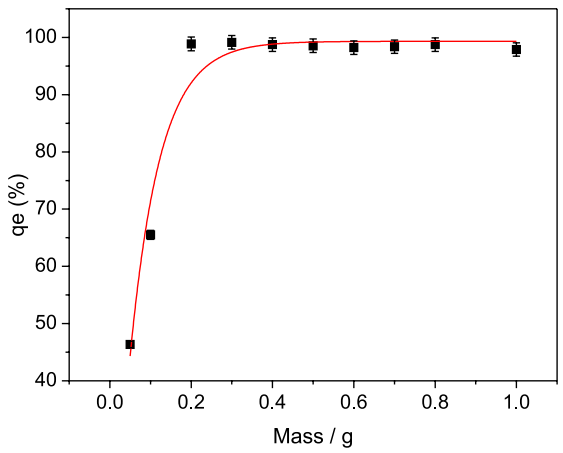

Figure 5. Adsorption of tartrazine dye on activated guava seed carbon (GSC) as a function of adsorbent dosage: C_0 = 20 mg L^{-1}, time = 3 h, initial pH = 6.10. C_0 is the initial concentration of the tartrazine dye solution.

pH study

The effect of pH on the ability of GSC to adsorb tartrazine dye is depicted in Table 3. Dye removal was not influenced by medium pH; thus, the kinetic study was carried out at the pH of the aqueous dye solution (pH = 6.10).

Tartrazine (trisodium-5-hydroxy-1-(4-sulfonatophenyl)-4-(4-sulfonato phenylazo)-*H*-pyrazole-3-carboxylate) is an anionic dye that, upon dissociation in aqueous medium, possesses three negatively charged groups, including two SO_3^- groups and one COO^- group. Therefore, the best adsorption rates were expected to occur at pH values below the pH_{pzc} of GSC (pH < 7.0), as functional groups present on the GSC surface would be protonated, resulting in electrostatic attraction with anionic groups of the dye molecule. However, the results demonstrated that the adsorption process was not governed by electrostatic attraction under the studied conditions. The adsorption behavior can be explained by other types of adsorbent-adsorbate interactions reported to participate in tartrazine adsorption, such as the formation of hydrogen bonds, van der Waals forces, and π-π interactions between π electrons of the adsorbent and π electrons of the aromatic ring dyes.[24,31,32]

Kinetic study

Adsorption kinetics were determined using an adsorbent mass of 0.3 g, and the pH was not adjusted, so that the suspension (adsorbent/adsorbate) maintained a condition close to that of the real system. Solutions were

Table 3. Effect of initial pH on the adsorption capacity of tartrazine dye on activated guava seed carbon (GSC): C_0[a] = 20 mg L^{-1}, mass = 0.3 g, time = 3 h

pH	Dye removal / %
2	98.04
3	98.28
5	98.16
7	97.91
9	98.16
10	98.16
11	98.16

[a]C_0: initial concentration of the tartrazine dye solution.

kept under stirring for 5 to 240 min at a mass/volume ratio of 0.3 g to 25 mL. The solute concentration was kept constant at 20 mg L^{-1}. The results of the kinetic study, described in Table S2 (SI section) and Figure 6a, showed that adsorption capacity increased with increasing contact time between adsorbent and adsorbate, until reaching equilibrium. In the initial stage (first 5 min), the amount adsorbed was 1.15 mg g^{-1}, representing a removal of 69.3%. This finding indicates that there was a greater number of available sites in the beginning, being rapidly occupied by tartrazine (5-dihydro-5-oxo-1(4-sulfophenyl)4-[4-sulfophenyl-azo]-1*H*-pyrazole-3-carboxylate). This behavior can be attributed to the rapid utilization of the most readily available adsorption sites on the surface of GSC.[33]

From 100 min onward, the variations were discrete, with an adsorbed amount of 1.61 mg g^{-1} (approximately 96.8% removal). Therefore, equilibrium had been reached. To confirm the equilibrium time and better describe dye adsorption on GSC, we generated a Southwell plot for the kinetic results. The findings are illustrated in Table S3 (SI section) and Figure 6b. The Southwell plot method consists of plotting a graph of time/amount adsorbed *vs.* time. The inverse of the slope of the fitted line indicates the value of q_e for the equilibrium point.[34,35]

The values of q_e for the entire experimental dataset are compared, and the equilibrium point is determined by analyzing the errors found at each point.

The results presented in Table S3 indicate that equilibrium was reached in under 100 min, as suggested in Figure 6b. From 50 min onward, the amount of dye adsorbed differed by less than 1% from that absorbed at 240 min, suggesting that tartrazine adsorption on GSC can reach an efficiency greater than 96% in less than 1 h. These findings are promising for future pilot-scale applications with real systems containing the dye, which is known to be toxic and recalcitrant.

After defining the equilibrium time, it was possible to model the adsorption kinetics of the activated carbon. Pseudo-first-order, pseudo-second-order, and Elovich models were tested. Model predictions were compared with experimental data (Figure 7), and the kinetic parameters were estimated (Table 4).

The Elovich kinetic model was adequate to describe the adsorption of dye on the adsorbent as shown by its correlation value (R^2), 0.983 (Table 4), suggesting the presence of chemical interactions associated with the effect of carbon surface heterogeneity on adsorption. This model indicates that adsorption occurs heterogeneously, with different activation energies for the process.[36] In the case of the GSC-tartrazine system, the greater value of α (49.85) compared with that of β (6.24) suggests that the adsorption rate was higher than that of desorption. Therefore, the proposed adsorption reaction is viable.

For comparison of the adsorption capacities of different adsorbents for tartrazine, it is necessary to consider factors possibly interfering with the efficiency of the system. Table 5 presents such a comparison, taking into account adsorbent dosage, concentration, equilibrium time, and removal efficiency. We highlight that GSC showed a

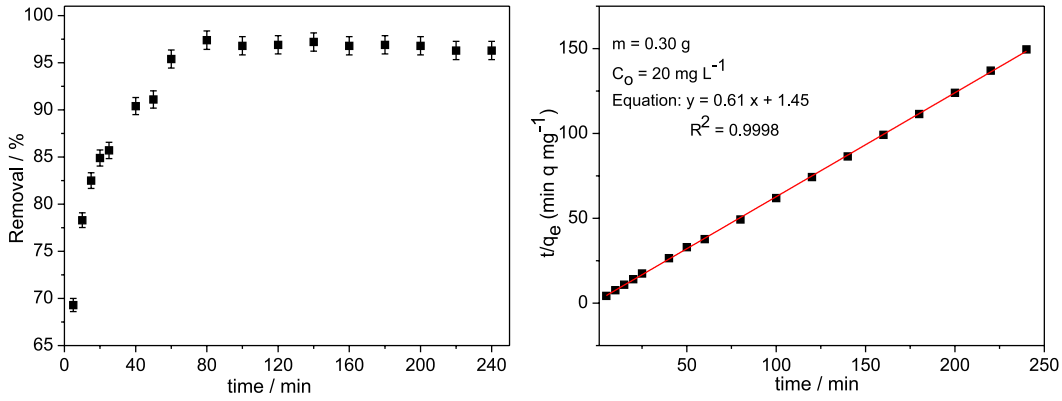

Figure 6. (a) Adsorption kinetics of tartrazine dye on activated guava seed carbon (GSC): C_0 = 20 mg L^{-1}, mass = 0.3 g, pH = 6.10 and (b) Southwell plot of the kinetic study. C_0 is the initial concentration of the tartrazine dye solution.

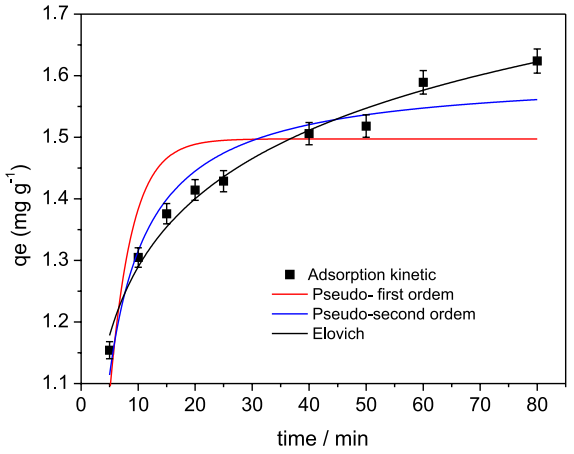

Figure 7. Comparison of pseudo-first-order, pseudo-second-order, and Elovich models for tartrazine dye adsorption on activated guava seed carbon (GSC), where q_e is the maximum sorption capacity of the adsorbent.

Table 4. Kinetic parameters for tartrazine dye adsorption on activated guava seed carbon (GSC) using different models

Kinetic model	Parameter	GSC
Pseudo-first-order	q_e / (mg g^{-1})	1.49
	K_{S1} / min^{-1}	0.26
	R^2	0.639
Pseudo-second-order	q_e / (mg g^{-1})	1.60
	K_{S2} / (g mg^{-1} min^{-1})	0.28
	R^2	0.923
Elovich	α / (mg g^{-1} min^{-1})	49.85
	β / (g mg^{-1})	6.24
	R^2	0.983

q_e: maximum sorption capacity of the adsorbent; K_{S1}: Lagergren rate constant of the pseudo-first-order; K_{S2}: adsorption rate constant of the pseudo-second-order; R^2: coefficient of determination; α and β are Elovich parameters (α = initial sorption rate and β = desorption constant).

comparable removal efficiency with other adsorbents (97.4%), with a good amount of adsorbed dye.

In this preliminary research whose objective was to evaluate the potential of guava seed in the preparation of carbon and its efficiency in removing tartrazine dye, the results obtained with removal above 90% and high surface area will be important for evaluating reuse cycles and their stability in future works.

Adsorbent materials not only must have a high adsorption capacity for contaminants but also need to be able to withstand several reuse cycles. These are key characteristics to reduce operational costs and minimize waste generation from secondary pollution.[24,32] Reusability depends on how easily adsorbent-adsorbate interactions can be disrupted without affecting adsorbent properties in successive adsorption cycles.[42,43] The selection of a desorption method depends on different factors, such as chemical characteristics of the adsorbent and the adsorbate and, mainly, the mechanism governing adsorbent-adsorbate interactions. Of note, pollutant adsorption can follow several different mechanisms.[42,43]

For systems similar to that developed here, regeneration methods typically consist of washing with different solvents to promote adsorbate desorption. For instance, aqueous solutions of NaOH (0.1 mol L^{-1}), NaCl (0.1 mol L^{-1}), HCl (0.1 mol L^{-1}), H_2SO_4 (0.1 mol L^{-1}), and H_3PO_4 (0.1 mol L^{-1}) were used to remove tartrazine from activated carbon.[24,32,43,44]

Conclusions

GSC, produced by a simple, low-cost method using guava seeds, was efficient in removing tartrazine from aqueous solutions. The lignocellulosic composition of guava favored the formation of a graphitic structure typical of carbonaceous materials, and activation with zinc chloride generated active sites for dye adsorption. Kinetic data were assessed using pseudo-first-order, pseudo-second-order, and Elovich models, and the latter two provided better fits, according to R^2 values. This finding suggests that chemisorption was the main mechanism and highlights the influence of the heterogeneous adsorbent surface on

Table 5. Comparison of activated guava seed carbon produced (GSC) and other adsorbent materials studied in the literature for the batch removal of tartrazine dye

Material	Adsorbent dosage / (g L^{-1})	C_0[a] / (mg L^{-1})	Equilibrium time / min	Removal / %	Reference
Activated guava seed carbon (GSC)	12	20	80	97.4[b]	this study
Layered double hydroxide (Zn_2Al/Cl-LDH)	0.4	20-240	60	96.83	37
Coconut shell	3-7	40-100	30	97–99	38
UiO-66@PVDF beads	0.8	40	120	97	39
Saw dust	5	15	70	71	40
Nanocomposite (KMCM)	2	100	180	n.r.[c]	41

[a]C_0: initial concentration of the tartrazine dye solution; [b]experimental value this study; [c]n.r.: not reported by the authors.

adsorption. The Southwell plot of the kinetic data showed that the equilibrium time was 80 min. The removal percentages after this period differed by less than 1%, showing that GSC achieved a tartrazine removal efficiency of more than 90% in less than 1 h. From an environmental point of view, the production of activated carbon from agro-industrial waste is an alternative to the inadequate disposal of solid waste. The good performance of GSC over a wide pH range indicated great potential for use in real systems, as it precludes the need for adjusting the medium pH. However, it is necessary to study the regeneration of this material to determine the feasibility of its application in wastewater treatment.

Supplementary Information

Supplementary material is available free of charge at http://jbcs.sbq.org.br as a PDF file.

Acknowledgments

This study was financed in part by the Coordenação de Aperfeiçoamento de Pessoal de Nível Superior - Brasil (CAPES) - Finance Code 001. The authors thank the Conselho Nacional de Desenvolvimento Científico e Tecnológico (grant No. 311419/2018-6) and the Financiadora de Estudos e Projetos (FINEP) for the financial support.

Author Contributions

Elinei N. C. Almeida was responsible for data curation, formal analysis, investigation, methodology, resources, validation, writing (original draft, review and editing); Erlan A. Pacheco for formal analysis, funding acquisition, investigation, methodology, software; Koji J. Nagahama for methodology, resources, software, writing (original draft, review and editing); Tereza S. M. Santos for conceptualization, data curation, formal analysis, funding acquisition, investigation, methodology, project administration resources, software supervision validation, visualization, writing (original draft, review and editing); Alexilda O. Souza for conceptualization, data curation, formal analysis, funding acquisition, investigation, methodology, project administration, resources, software, supervision, validation, visualization, writing (original draft, review and editing).

References

1. Dai, Y.; Zhang, N.; Xing, C.; Cui, Q.; Sun, Q.; *Chemosphere* **2019**, *223*, 12. [Crossref]
2. Natarajan, S.; Bajaj, H. C.; Tayade, R. J.; *J. Environ. Sci*. **2017**, *65*, 201. [Crossref]
3. Ewis, D.; Ba-Abbad, M. M.; Benamor, A.; El-Naas, M. H.; *Appl. Clay Sci*. **2022**, *229*, 106686. [Crossref]
4. Lan, D.; Zhu, H.; Zhang, J.; Li, S.; Chen, Q.; Wang, C.; Wu, T.; Xu, M.; *Chemosphere* **2021**, *293*, 133464. [Crossref]
5. Basu, S.; Ghosh, G.; Saha, S.; *Process Saf. Environ. Prot.* **2018**, *117*, 125. [Crossref]
6. Benhachem, F. Z.; Attar, T.; Bouabdallah, F.; *Chem. Rev. Lett*. **2019**, *2*, 33. [Crossref]
7. Hamzezadeh, A.; Rashtbari, Y.; Afshin, S.; Morovati, M.; Vosoughi, M.; *Int. J. Environ. Anal. Chem.* **2020**, *102*, 254. [Crossref]
8. Sultana, M.; Rownok, M. H.; Sabrin, M.; Rahaman, M. H.; Alam, S. M. N.; *Clean. Eng. Technol*. **2022**, *6*, 100382. [Crossref]
9. Singare. P. U.; *J. Environ. Chem. Eng.* **2019**, *7*, 102899. [Crossref]
10. Geng, Y.; Zhang, J.; Zhou, J.; Lei, J.; *RSC Adv*. **2018**, *8*, 32799. [Crossref]
11. Leal, T. W.; Lourenço, L. A.; Scheibe, A. S.; de Souza, S. M. A. G. U.; de Souza, A. A. U.; *J. Environ. Chem. Eng*. **2018**, *6*, 2705. [Crossref]
12. Chauhan, P. R.; Raveesh, G.; Pal, K.; Goyal, R.; Tyagi, S. K.; *Bioresour. Technol. Rep.* **2023**, *22*, 101425. [Crossref]
13. Dutta, S.; Gupta, B.; Srivastava, S. K.; Gupta, A. K.; *Mater. Adv.* **2021**, *2*, 4497. [Crossref]
14. Omo-Okoro, P. N.; Adegbenro, P. D.; Okonkwo, J. O.; *Environ. Technol. Innovation* **2018**, *9*, 100. [Crossref]
15. Tian, D.; Xu, Z.; Zhang, D.; Chen, W.; Cai, J.; Deng, H.; Sun, Z.; Zhou, Y.; *J. Solid State Chem.* **2019**, *269*, 580. [Crossref]
16. Blanchnio, M.; Derylo-Marczewska, A.; Charmas, B.; Zienkiewicz-Strzalka, M.; Bogatyrov, V.; Galaburda, M.; *Molecules* **2020**, *25*, 5105. [Crossref]
17. Lewoyehu, M.; *J. Anal. Appl. Pyrolysis* **2021**, *159*, 105279. [Crossref]
18. Pallarés, J.; González-Cencerrado, A.; Arauzo, I.; *Biomass Bioenergy* **2018**, *115*, 64. [Crossref]
19. Martínez, R. J.; Vela-Carrillo, A. Z.; Godínez, L. A.; Pérez-Bueno, J. J.; Robles, I.; *Biomass Bioenergy* **2023**, *168*, 106660. [Crossref]
20. Mo, J.; Yang, Q.; Zhang, N.; Zhang, W.; Zheng, Y.; Zhang, Z.; *J. Environ. Manage.* **2018**, *227*, 395. [Crossref]
21. Vela-Carrillo, A. Z.; Martínez, R. J.; Godínez, L. A.; Pérez-Bueno, J. D. J; Espejel-Ayala, F.; Robles, I.; *Biomass Convers. Biorefin.* **2022**, *14*, 733. [Crossref]
22. Gomez-Delgado, E.; Nunell, G.; Cukierman, A. L.; Bonelli, P.; *Bioresour. Technol. Rep.* **2022**, *18*, 101008. [Crossref]
23. da Costa, W. K. O. C.; Gavazza, S.; Duarte, M. M. M. B.; Freitas, S. K. B.; Paula, N. T. G.; Paim, A. P. S.; *Water, Air, Soil Pollut*. **2021**, *232*, 358. [Crossref]
24. Rzig, B.; Kojok, R.; Khalifa, E. B.; Magnacca, G.; Lahssini, T.; Hamrouni, B.; Bellakhal, N.; *Biomass Convers. Biorefin.* **2023**, 1. [Crossref]

25. Ho, Y.-S.; *J. Hazard. Mater.* **2006**, *136*, 681. [Crossref]
26. Mohammadi, S. Z.; Karimi, M. A.; Afzali, D.; Mansouri, F.; *Desalination* **2010**, *262*, 86. [Crossref]
27. Gupta, S. S.; Bhattacharyya, K. G.; *Adv. Colloid Interface Sci.* **2011**, *162*, 39. [Crossref]
28. Selvaraju, G.; Bakar, N. K. A.; *J. Cleaner Prod.* **2017**, *141*, 989. [Crossref]
29. Islam, M. S.; Ang, B. C.; Gharehkhani, S.; Afifi, A. B. M.; *Carbon Lett.* **2016**, *20*, 1. [Crossref]
30. Thommes, M.; Kaneko, K.; Neimark, A. V.; Olivier, J. P.; Rodriguez-Reinoso, F.; Rouquerol, J.; Sing, K. S.; *Pure Appl. Chem.* **2015**, *87*, 1051. [Crossref]
31. Paredes-Laverde, M.; Salamanca, M.; Diaz-Corrales, J. D.; Flórez, E.; Silva-Agredo, J.; Torres-Palma, R. A.; *J. Environ. Chem. Eng.* **2021**, *9*, 105685. [Crossref]
32. Micheletti, D. H.; da Silva Andrade, J. G.; Porto, C. E.; Alves, B. H. M.; de Carvalho, F. R.; Sakai, O. A.; Batistela, V. R.; *Bioresour. Technol. Rep.* **2023**, *24*, 101598. [Crossref]
33. Pehlivan, E.; Kahraman, H. T.; *Food Chem.* **2012**, *133*, 1478. [Crossref]
34. Bernat-Maso, E.; Lluis, G.; Roca, P.; *Constr. Build. Mater.* **2014**, *73*, 180. [Crossref]
35. de Almeida, M. L. S.; Lima, A. C. P.; Nagahama, K. J.; Santos, T. S. M.; *J. Contam. Hydrol.* **2021**, *242*, 103841. [Crossref]
36. Khan, T. A.; Sharma, S.; Khan, E. A.; Mukhlif, A. A.; *Toxicol. Environ. Chem.* **2014**, *96*, 555. [Crossref]
37. Mahmoud, M. E.; Abdelfattah, A. M.; Tharwat, R. M.; Nabil, G. M.; *J. Mol. Liq.* **2020**, *318*, 114297. [Crossref]
38. Tejada-Tovar, C.; Villabona-Ortiz, À.; Aguilar-Bermúdez, F.; Pájaro-Moreno, Y.; González-Delgado, A. D.; *Processes* **2023**, *11*, 3115. [Crossref]
39. Singh, H.; Goyal, A.; Bhardwaj, S. K.; Khatri, M.; Bhardwaj, N.; *J. Mater. Sci. Eng. B* **2023**, *288*, 116165. [Crossref]
40. Banerjee, S.; Chattopadhyaya, M. C.; *Arabian J. Chem.* **2017**, *10*, S1629. [Crossref]
41. Amaku, J. F.; Taziwa, R.; *Sci. Rep.* **2023**, *13*, 9872. [Crossref]
42. Alcade-Garcia, F.; Prasher, S.; Kaliaguine, S.; Tavares, J. R.; Dumont, M. J.; *ACS Eng. Au.* **2023**, *3*, 443. [Crossref]
43. Amaku, J. F.; Oyedotun, K. O.; Maxakato, N. W.; Akpomie, K. G.; Okeke, E. S.; Olisah, C.; Malloum, A.; Adegoke, K. A.; Ighalo, J. O.; Conradie, J.; Ohoro, C. R.; *Chem. Africa* **2024**, *7*, 1685. [Crossref]
44. Fennouh, R.; Benturki, O.; Mokhati, A.; Benturki, A.; Belhamdi, B.; Trari, M.; *Biomass Convers. Biorefin.* **2023**, *14*, 16171. [Crossref]

Submitted: January 24, 2024
Published online: July 24, 2024